Indonesian Journal of Environmental Management and Sustainability
e-ISSN:2598-6279 *p*-ISSN:2598-6260

IJEMS

Research Paper

AERMOD as an Alternative Approach for Estimating Traffic-Related Ambient Pollutant Dispersion in Areas Without Air Quality Monitoring Stations

Gian Mustika Ilmi[1], Vera Surtia Bachtiar[1*], Yumita Sufitri[1], Shinta Silvia[1] and Reri Afrianita[1]

[1] *Environmental Engineering, Universitas Andalas, Padang, West Sumatra, 25163, Indonesia*
***Corresponding author e-mail**: verasurtia@eng.unand.ac.id

Abstract

The dispersion of pollutants originating from traffic activities has become a major environmental issue in many developing countries. Emissions such as SO_2 and CO present significant challenges for air quality management due to their serious health impacts. Air Quality Monitoring Systems (AQMS) are commonly used to measure pollutant concentrations; however, limited availability and spatial coverage necessitate alternative approaches such as dispersion modeling using AERMOD. This study aims to evaluate the performance of AERMOD as an alternative method for estimating SO_2 and CO concentrations, particularly those associated with traffic-related emissions. The simulation results indicate a strong alignment between dominant wind direction and pollutant dispersion patterns over the seven-day modeling period. Concentration accuracy assessed through regression analysis and Root Mean Square Error (RMSE) revealed positive correlations between AERMOD simulations and observational data for both SO_2 and CO, with RMSE values of 21.86 $\mu g/m^3$ for SO_2 and 485.25 $\mu g/m^3$ for CO. Overall, statistical evaluations demonstrate a high level of agreement for SO_2 and a moderate level of agreement for CO. These findings underscore the significant potential of AERMOD as an alternative monitoring tool for estimating pollutant dispersion in areas lacking AQMS infrastructure, thereby supporting more effective air quality management and pollution control strategies. However, the model's performance remains influenced by several limitations, including dependency on the quality of meteorological and emission input data, the assumption of steady-state atmospheric conditions, and greater prediction uncertainty for CO compared to SO_2. These factors should be carefully considered when applying AERMOD in regions without ground-based monitoring stations.

Keywords

Dispersion, Modeling, AERMOD, Air Quality Monitoring System (AQMS), SO_2, CO

Received: 25 October 2025, Accepted: 4 January 2026
https://doi.org/10.26554/ijems.2026.10.1.1-16

1. INTRODUCTION

One of the major environmental challenges commonly faced by developing countries is air pollution resulting from anthropogenic sources, particularly emissions from the transportation sector and industrial activities. In developing countries, the transportation sector is one of the primary contributors to urban air pollution. This sector emits a substantial proportion of hazardous pollutants, including particulate matter ($PM_{2.5}$ and PM_{10}), toxic gases (NO_x, CO, SO_2, and black carbon), as well as greenhouse gases such as CO_2. In several major cities, road transportation alone can contribute up to 50% of total air pollutants, particularly nitrogen dioxide (NO_2) and particulate matter in areas with high vehicular density. This issue is further exacerbated by rapid urbanization, increased reliance on private vehicles, and the large proportion of aging, poorly maintained vehicles in operation (Colvile et al., 2001; Herath Bandara and Thilakarathne, 2025; Kiribou et al., 2025; Singh et al., 2021).

A comprehensive systematic review published in 2022 by John Wiley & Sons quantitatively confirmed the association between exposure to specific air pollutants and multiple health outcomes. The review evaluated 101 epidemiological studies spanning four decades and demonstrated a significant correlation between exposure to Sulfur Dioxide (SO_2) and the incidence of Chronic Obstructive Pulmonary Disease (COPD) as well as cardiovascular disorders. Moreover, exposure to Carbon Monoxide (CO) was also linked to an increased risk of Parkinson's disease and cardiovascular complications, until mortality providing robust empirical evidence of the global health impacts of air pollution (Chen et al., 2007, 2022; Sobieraj et al., 2022; Xu et al., 2021).

In response to the significant health risks posed by SO_2

and CO, the implementation of various control and monitoring techniques has become a primary priority. One of the key approaches to air quality monitoring is the use of an Air Quality Monitoring System (AQMS), which offers the advantage of providing real-time data. The Air Quality Monitoring System (AQMS) is designed to continuously measure the ambient concentrations of several pollutants, such as CO and SO_2, in real time. It has been widely implemented for diverse applications, including the monitoring of industrial emissions in compliance with prevailing Environmental Protection Agency (EPA) regulations (Zheng, 2009; Kumar et al., 2021). This system typically measures a range of parameters, including oxygen, carbon monoxide, carbon dioxide, nitrogen oxides, sulfur compounds, hydrocarbons, temperature, humidity, and noise levels, using electrochemical and electromechanical sensors (Hussain et al., 2020; Kumar et al., 2011).

The distribution of Air Quality Monitoring Systems (AQMS) in most developing countries is generally limited, uneven, and accompanied by various challenges. Many nations, particularly those in South Asia, Southeast Asia, and Africa, have an insufficient number of monitoring stations relative to their population size. For instance, countries such as Sri Lanka and Myanmar are significantly under-equipped with AQMS units compared to the required number for adequate coverage. Although other nations, including Indonesia and Malaysia, possess more extensive networks, they still face disparities in terms of station density when measured against the ideal coverage criteria necessary for comprehensive air quality monitoring (Verma et al., 2023). In addition, effective AQMS siting requires the strategic placement of monitoring stations to ensure broad spatial coverage, capture pollution variability, and maintain cost efficiency (Ajnoti et al., 2024; Hura and Dutsiak, 2024). Given the inherent limitations of these monitoring instruments, it is essential to identify alternative solutions capable of predicting the spatial distribution of pollutants more uniformly across wider regions, rather than being restricted to specific monitoring locations.

One of the air-dispersion models recommended by the United States Environmental Protection Agency (EPA) is AERMOD, which is among the most widely used tools for simulating the dispersion of air pollutants. The model is particularly suitable for applications in urban environments within a range of up to 50 km and is capable of processing multiple emission sources simultaneously up to ten sources in a single run. Studies by Jittra et al. (2015) and Thepanond (2016) reported that AERMOD provides better predictive performance than other models such as CALPUFF, especially in densely populated regions. Furthermore, a comprehensive evaluation conducted in Delhi demonstrated that AERMOD exhibits lower predictive bias compared to the ADMS-Urban model (Mohan et al., 2011). However, several studies also indicate that AERMOD tends to overestimate pollutant concentrations particularly NO_2 and particulate matter when compared with observational monitoring data. For example, in Kigali, Rwanda, AERMOD predicted an annual mean NO_2 concentration of 50.4 $\mu g/m^3$, substantially higher than the observed range of 15–20 $\mu g/m^3$, although some statistical indices still suggested moderate agreement (Craig et al., 2020; Demirarslan, 2025; Irankunda et al., 2022).

This study focuses on the specific analysis of gaseous parameters, namely carbon monoxide (CO) and sulfur dioxide (SO_2), due to the availability of AQMS data and the relevance of vehicle-specific emission factors for these pollutants. The primary objective of this research is to validate the predicted results generated by the AERMOD dispersion model using actual data obtained from AQMS in order to evaluate the model accuracy. This study also addresses common challenges in ambient air quality measurements, particularly the accuracy of results influenced by meteorological conditions and the placement of monitoring instruments. To mitigate potential inaccuracies arising from the positioning of AQMS stations that may not align with the prevailing wind direction, direct measurements were conducted using a gas impinger sampler. Ultimately, these direct measurements are compared with both AERMOD predictions and AQMS data to provide a more comprehensive evaluation of ambient air quality. The findings are expected to demonstrate the reliability of AERMOD as a feasible predictive tool for pollutant dispersion analysis in regions lacking AQMS infrastructure.

2. EXPERIMENTAL SECTION

2.1 Methods

2.1.1 Study Area

The modeling area focused on Jenderal Sudirman Street, one of the main and busiest corridors in Padang City, as shown in Figure 1. This corridor serves as a central business and administrative zone and is considered representative of typical urban traffic conditions, making it suitable for assessing CO and SO_2 concentrations emitted by motor vehicles. To capture variations during peak and off-peak hours, sampling was conducted across four time periods Morning (07:00–08:00), Afternoon (12:00–13:00), Evening (16:00–17:00), and Night (20:00–21:00) for one full week from May 5, 2025, to May 12, 2025. The modeling area covered approximately 600 meters, stretching from point A to point B, which was selected based on consistent traffic characteristics.

2.2 Data Collection

2.2.1 Traffic Activity

Traffic activity along the Jenderal Sudirman corridor from point A to point B (as shown in the Figure 1) was observed to obtain vehicle volume data categorized by vehicle type. Counts were conducted during four time periods, Morning (07:00–08:00), Afternoon (12:00–13:00), Evening (16:00–17:00), and Night (20:00–21:00), in order to capture

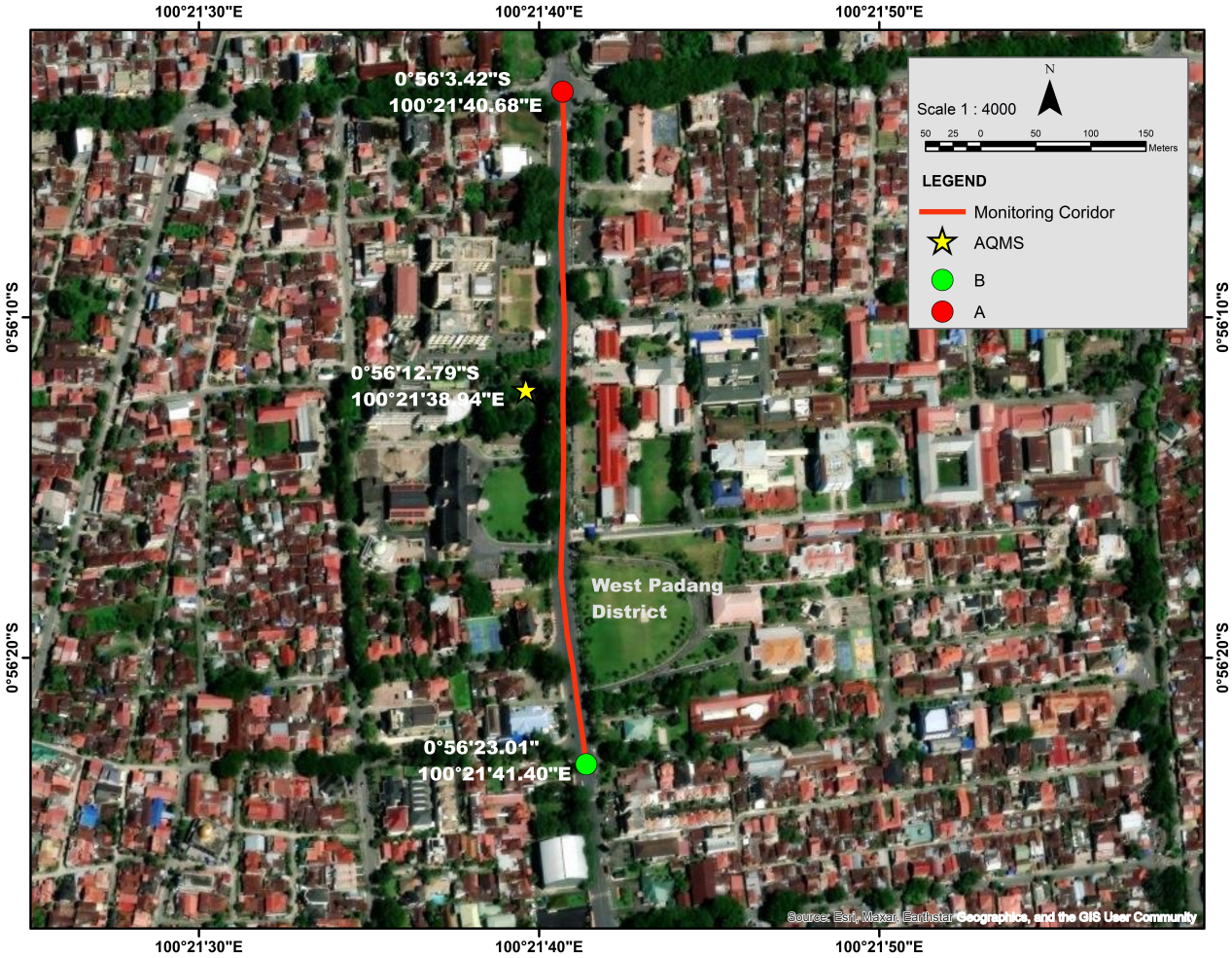

Figure 1. Site Location

variations in traffic during peak and off-peak hours over a full week, from 5 May 2025 to 12 May 2025. The resulting data are presented in Table 1. The selection of these time intervals and observation duration was intended to capture both intra-day and inter-day traffic variability, ensuring that the collected data are sufficiently representative for emission modeling purposes.

2.2.2 Meteorological Data

Meteorological parameters are fundamental variables that critically influence dispersion mechanisms and determine the variability of atmospheric pollutant concentrations. Specifically, factors such as wind speed, temperature, atmospheric pressure, and humidity collectively exert distinct effects on pollutant concentration fluctuations (Qi et al., 2021). Therefore, the accuracy of meteorological parameters is essential as input data for the AERMET processor within the AERMOD modeling framework. Given the importance of high temporal resolution particularly hourly data in dispersion modeling, and the limited availability of ground-based observational datasets, satellite-derived data serve as an effective alternative source.

This study utilizes meteorological data from NASA POWER, which provides global datasets at multiple temporal

Table 1. Traffic Activity Data Based on Time Periods Over a One-Week Interval

Category	Morning	Afternoon	Evening	Night
Motorcycle	12113	10710	11137	12276
Car	8154	11699	8997	8182
Bus	144	165	88	106
Truck	68	155	128	57
Public Minibus	89	80	69	8
Taxi	24	37	42	36
Pick Up	124	323	220	163
Van/Minibus	104	233	167	159
Sedan	237	227	248	216
Pedicab	104	97	136	53
Jeep	50	45	40	43

resolutions including hourly, daily, and monthly at a spatial resolution of 1° × 1° latitude/longitude, publicly accessible through the POWER data portal (Chandler et al., 2013). NASA POWER relies on meteorological reanalysis products, such as MERRA-2 (Modern Era Retrospective analysis for Research and Applications, Version 2), which are further processed through linear temporal interpolation to obtain hourly values under the assumption of gradual atmospheric changes between intervals. Temperature, humidity, and pressure variables were interpolated linearly, while wind speed and wind direction were adjusted through bias correction and temporal disaggregation based on characteristic diurnal patterns of tropical urban climates, ensuring that short-term fluctuations are better represented (Aboelkhair et al., 2019). The daily mean meteorological parameters observed during the monitoring period are presented in Table 2.

2.2.3 Gas Impinger Sampler

The pollutant concentration was measured directly using a gas impinger sampler (Figure 2) in accordance with the determination of the sample location point using the Indonesian National Standard (SNI) 19-7119.9-2005, while for the field measurement method using (SNI) 7119-5:2017. The sampling process was conducted over seven consecutive days during four intervals, Morning (07:00–08:00 WIB), Afternoon (12:00–13:00 WIB), Evening (16:00–17:00 WIB), and Night (20:00–21:00 WIB), consistent with the real time monitoring schedule of the AQMS.

Figure 2. Gas Impinger Sampler

2.2.4 Air Quality Monitoring System (AQMS)

Real time CO and SO_2 concentration data from the Air Quality Monitoring System (AQMS) located around Jalan Sudirman were used to validate the AERMOD simulation results. The AQMS records pollutant concentrations at regular intervals, enabling the capture of temporal variations during peak and nonpeak periods, Figure 3 shows the AQMS unit used in this study. In general, an AQMS consists of air sensors, a data processing unit, communication modules, a power supply, and software for data transmission, visualization, and analysis (Suhito et al., 2020). The system measures key pollutants such as CO and SO_2 and sends the processed data in real time to a central server, providing reliable reference values for model validation.

The Air Quality Monitoring System (AQMS) used in this study was a TRUSUR®AQM instrument permanently installed at an air quality monitoring station. The system employs active sampling using a diaphragm pump with a controlled flow rate (±0.9 L/min) to ensure measurement stability. Concentrations of CO, SO_2, NO_2, and O_3 were measured using electrochemical sensors characterized by linear response, repeatability better than 2%, response times of 20–60 s, and long-term drift of less than 2% per month. The system supports manual zero and span calibration using certified standard gases, which is recommended to be performed every six months. AQMS data were used as supporting observational data to evaluate the spatial and temporal patterns of dispersion model results, while acknowledging the measurement uncertainty associated with nonreference-grade instruments.

2.3 Emission Estimation

The emission load from motor vehicle activity along Jenderal Sudirman Street, Padang City, was estimated using an emission inventory calculation approach commonly applied in transportation and air pollution studies. The initial step involved determining traffic volume to obtain traffic intensity, where volume (V) is calculated as the number of vehicles (n) per unit time (t), following Tamin (2008):

$$V = \frac{n}{t} \tag{1}$$

To quantify pollutant emissions, this study employed a scenario-based modeling approach in which traffic activity was evaluated during four observation periods morning, afternoon, evening, and night to represent peak and off-peak traffic conditions. A baseline traffic emission scenario was applied to represent actual traffic conditions during the observation period. Emission factors were assumed to be constant for each vehicle category and applied uniformly over the simulation period in accordance with national regulations. Hourly traffic volumes were used to derive time-dependent emission rates, which were converted into line source inputs (g/s) for the AERMOD model. The total emission estimates

Table 2. Daily Average Values of Observed Meteorological Parameters

Parameters	Daily Mean Meteorological Data						
	5/5/25	5/6/25	5/7/25	5/8/25	5/9/25	5/10/25	5/11/25
Wind Speed (m/s)	2.23	2.14	2.14	3.23	3.20	3.37	3.77
Wind Direction (degree)	245.52	203.45	217.00	251.09	232.30	252.69	260.51
Temperature (°C)	24.33	25.21	25.29	24.75	24.59	23.94	23.76
Humidity (%)	88.04	85.91	87.53	89.07	87.38	90.77	92.91
Pressure (kPa)	94.86	94.83	94.75	94.81	94.87	94.86	94.78
Precipitation (mm/day)	1.50	0.75	1.21	1.99	4.30	1.57	4.85
Radiation (Wh/m^2)	227.64	233.48	226.32	188.70	209.99	199.29	161.85
Cloud Cover (Dimensionless Fraction)	0.81	0.88	0.91	0.97	0.98	0.90	0.99

Source: NASA POWER Climate Data, NASA LaRC, 2025

Table 3. AERMOD Input Data Configuration

Parameter Group	Configuration Details
Model Version	AERMOD v8.9.0
Simulation Type	Steady-state Gaussian plume model
Study Domain	Urban area, radius 50 km from emission source
Meteorological Data	NASA POWER data meteorology (May 5, 2025 – May 12, 2025), upper air estimator, processed using AERMET
Surface Characteristics	Surface roughness length (z_0): 1 m; Albedo: 0.20; Bowen ratio: 1.62
Terrain Processing	Elevation processed using AERMAP; resolution: 30 m (SRTM)
Emission Source Type	Line source (roadway)
Emission Source Parameters	Traffic based emission rate (g/s), Base elevation, Release height, width and X, Y coordinate
Receptor Grid	Cartesian grid, spacing: 6 m
Averaging Period	1-hour concentration averages
Pollutants Modeled	SO_2 and CO
Output Format	Concentration contours ($\mu g/m^3$)
Model Assumptions	Flat and complex terrain

were based on the principle that emissions are the product of the emission factor (EF) and vehicle activity (n), in this study, the EF values for SO_2 and CO_2 were adopted from the Emission Factors contained in Minister of Environment Regulation Number 12 of 2010 concerning the Implementation of Regional Air Pollution Control, which provides standard emission factors for light vehicles, motorcycles, and diesel vehicles (Ministry of Enviroment, 2010).

Subsequently, total emissions were estimated based on the principle that emissions are the product of the emission factor (EF) and vehicle activity (n), as outlined in the EPA (2019) guidelines and the EMEP/EEA (2023) emission inventory manual. Accordingly, the emission load (E) was computed using the following equation:

$$E = EF \times n \tag{2}$$

2.4 Model Setup

In this study, the AERMOD dispersion model software was used to simulate pollutant distribution within the study area. AERMOD is an atmospheric dispersion model developed by the United State Environmental Protection Agency (EPA) in collaboration with the American Meteorological Society (AMS), designed to predict pollutant concentrations in urban environments. The model operates by integrating meteorological data and topographical characteristics to estimate pollutant concentrations at predefined receptor locations (Cimorelli et al., 2005).

Air dispersion modeling was conducted using the AERMOD model version 8.9.0 developed by the U.S. Environmental Protection Agency (EPA). AERMOD is a publicly available Gaussian plume dispersion model that can be freely accessed from official EPA repositories. The model was applied following standard AERMOD configuration procedures, including the use of appropriate meteorological preprocessing and source characterization. The use of a publicly available model ensures the reproducibility of the simulations.

The AERMOD modeling system consists of two primary preprocessors AERMET and AERMAP Figure 4. AERMET

Figure 3. Air Quality Monitoring Sampling (AQMS)

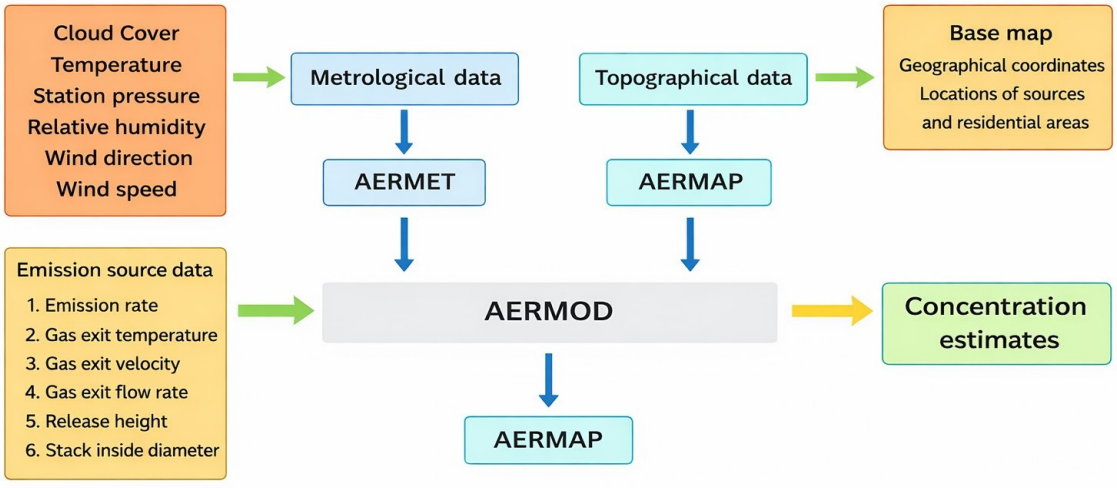

Figure 4. Workflow Diagram of the AERMOD Modeling System

processes meteorological inputs along with surface parameters such as albedo, Bowen ratio, and surface roughness, while AERMAP processes topographic data to determine the elevations of emission sources and receptor points (Cimorelli et al., 2005). AERMOD has been widely applied to assess pollutant dispersion from transportation activities in areas with high traffic density (Snyder et al., 2013). The modeling configuration applied in this study is presented in Table 3 and serves as the basis for generating the required simulation outputs.

2.5 Model Validation and Analysis

To evaluate the accuracy of the pollutant concentrations generated by the model, a validation process was conducted by comparing the AERMOD outputs with actual field measurements. Observational data were obtained from two sources secondary data from the Air Quality Monitoring System (AQMS), which provides continuous concentration measurements, and direct field measurements using the Impinger method. The simulation outputs were subsequently validated using observational data from AQMS and field measurements. To evaluate the model's performance for

SO_2 and CO, statistical indicators such as Pearson, Mean Absolute Error (MAE), (Root Mean Square Error) RMSE, and (Normalized Mean Square Error) NMSE were employed to assess both the linear relationship and the accuracy between the modeled results and actual observations. This approach ensures that the interpretation of results is not solely dependent on AERMOD outputs, but also reflects the quality of the input data and the model's ability to represent real-world conditions.

3. RESULTS AND DISCUSSION

3.1 Pollutant Concentrations

3.1.1 Atmospheric Environmental Research Model (AERMOD)

Dispersion modeling using the AERMOD software serves as an effective method for predicting pollutant concentrations in areas not yet covered by automatic air quality monitoring stations (AQMS). Based on this approach, the predicted concentrations and dispersion patterns of SO_2 and CO within the Jalan Sudirman study area are presented and analyzed.

The seven-day AERMOD simulation of SO_2 Figure 5(a) and CO Figure 5(b) concentrations reveals pronounced diurnal variability driven by the combined influence of traffic activity and meteorological conditions. SO_2 levels remain consistently elevated during the morning (>130 $\mu g/m^3$) and decrease toward the afternoon and evening (<140 $\mu g/m^3$), closely aligning with daily traffic intensity patterns. In contrast, CO exhibits a much wider concentration range (0–2300 $\mu g/m^3$), with peak values occurring at midday (1300–2300 $\mu g/m^3$), followed by the morning period (3–2200 $\mu g/m^3$), indicating a substantial contribution from rush-hour emissions. CO concentrations subsequently decline and stabilize during the afternoon–evening period (900–1800 $\mu g/m^3$).

Overall, peak concentrations for both pollutants occur predominantly in the morning, a pattern strongly associated with the formation of a thermal inversion layer resulting from the slow increase in surface temperature after sunrise. This inversion traps pollutants near the ground, leading to accumulation and elevated concentrations (Verma et al., 2023). The SO_2 and CO heatmap as shown in the Figure 5(a)-(b), dominated by yellow–red gradients, further reinforces the persistence of elevated concentrations across most observation periods.

A notable anomaly appears on the seventh day, when morning SO_2 concentrations decrease sharply to <1 $\mu g/m^3$, coinciding with the implementation of the weekly Car Free Day (CFD), which substantially reduces transportation-related emissions. These findings underscore that pollutant dispersion dynamics are strongly influenced by meteorological conditions, urban surface roughness characteristics (Kumar et al., 2006; Rezaali et al., 2025) the dominant contribution of the transportation sector as the primary source of SO_2 emissions in the study area.

3.1.2 Air Quality Monitoring System (AQMS)

The utilization of AQMS enables continuous recording of pollutant concentrations, allowing the identification of daily fluctuation patterns. Temporal dynamics supports the monitoring of short-term atmospheric conditions while also highlighting the contribution of motor vehicle emissions to ambient pollutant levels.

The analysis of daily trends in the Figure 6. reveals a consistent diurnal variation pattern for both primary pollutants, SO_2 and CO, during the first six days of observation. Their concentrations reached peak values during the morning period. SO_2 levels ranged between 130–135 $\mu g/m^3$, with the highest peak occurring on Day 2, while CO concentrations remained relatively stable above 1500 $\mu g/m^3$. The morning increase in pollutant levels is influenced by two primary mechanisms, high traffic intensity during peak commuting hours and the presence of a shallow boundary layer. A lower boundary layer limits vertical mixing, thereby enhancing the accumulation of pollutants from transportation activities (Lee et al., 2019; Su et al., 2018).

In contrast, pollutant concentrations during the midday and afternoon periods showed a marked decline, with SO_2 decreasing to 119–122 $\mu g/m^3$ and CO reduced to 600–750 $\mu g/m^3$. This decline reflects the dominant influence of surface heating, which increases boundary layer thickness and enhances turbulence, thereby accelerating dilution and vertical transport of pollutants (Oke et al., 2017; Stull, 1988). At night, SO_2 and CO concentrations increased again to moderate levels, ranging from 124–126 $\mu g/m^3$ and 1090–1219 $\mu g/m^3$. This condition indicates a more stable atmosphere with minimal turbulence, although traffic volume declines during nighttime, dispersion processes remain limited due to strong atmospheric stability that promotes near-surface pollutant retention (Oke et al., 2017; Stull, 1988).

A notable anomaly occurred on the seventh day for both pollutants, likely associated with a substantial reduction in traffic activity due to the implementation of Car Free Day within the observation area. The heatmap visualization Figure 6(a) and Figure 6(b) (right) reinforces the interpretation of these diurnal patterns. Dominant red–orange hues during morning hours across the first six days signify elevated concentrations, whereas the blue–green colors during midday and afternoon reflect enhanced dispersion efficiency driven by increased mixing layer development.

3.1.3 Empirical Measurement

The direct field measurements of SO_2 and CO concentrations exhibit clear and consistent temporal variations throughout the seven-day observation period, showing strong agreement with both the AERMOD simulations and AQMS observations Figure 7.

The concentrations of both pollutants exhibit pronounced morning peaks, with SO_2 consistently reaching 130–135 $\mu g/m^3$ Figure 7(a), while CO dominates with values exceeding 1500 $\mu g/m^3$ Figure 7(b), which is more than twice the

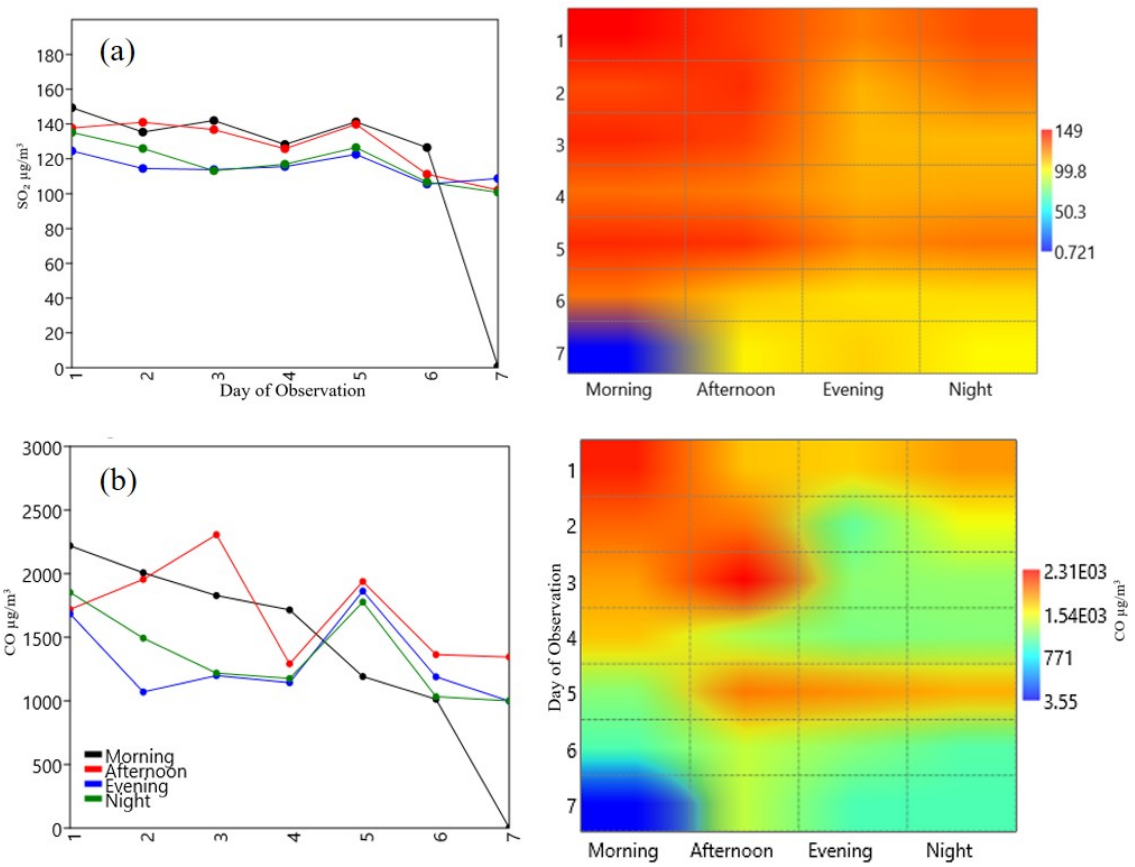

Figure 5. Distribution Variation and Heat Map of Daily Concentration Distribution Pattern Based on AERMOD (a) Sulfur Dioxide (SO_2) (b) Carbon Monoxide (CO)

Table 4. Model Validation Metrics for SO_2 and CO: AERMOD vs. AQMS and Empirical Measurements

	AERMOD and AQMS		AERMOD and Empirical Measurements	
	SO_2	CO	SO_2	CO
Pearson	0.60397	0.30428	0.61704	0.30514
p-value	0.00066582	0.20132	0.0006497	0.20097
MAE	13.7	695.17	13.686	696.7
NMSE	0.0378	0.3465	0.0378	0.3465
RMSE	21.869	485.22	21.592	485.25

concentrations observed during the midday and afternoon periods. These persistent peaks reflect typical traffic-related emission patterns during morning rush hours, further exacerbated by unfavorable meteorological conditions such as shallow mixing layers, a phenomenon commonly reported in developing countries (Tun et al., 2018). In contrast, pollutant concentrations decrease sharply during the midday and afternoon, reaching minimum levels for SO_2 (119–122 $\mu g/m^3$) and CO (600–750 $\mu g/m^3$), indicating more efficient dispersion driven by enhanced vertical mixing induced by solar heating.

During the nighttime period, concentrations stabilize at intermediate levels, with SO_2 ranging between 124–126 $\mu g/m^3$ and CO between 1025–1200 $\mu g/m^3$, reflecting the increased atmospheric stability that restricts dispersion processes. This behavior is consistent with previous findings showing that pollutant levels often rise under stable nocturnal conditions (Dobson et al., 2021). A notable anomaly is observed on Day 7 (Sunday), where both pollutants show a substantial decline, highlighting the strong influence of reduced vehicular activity associated with the Car Free Day event.

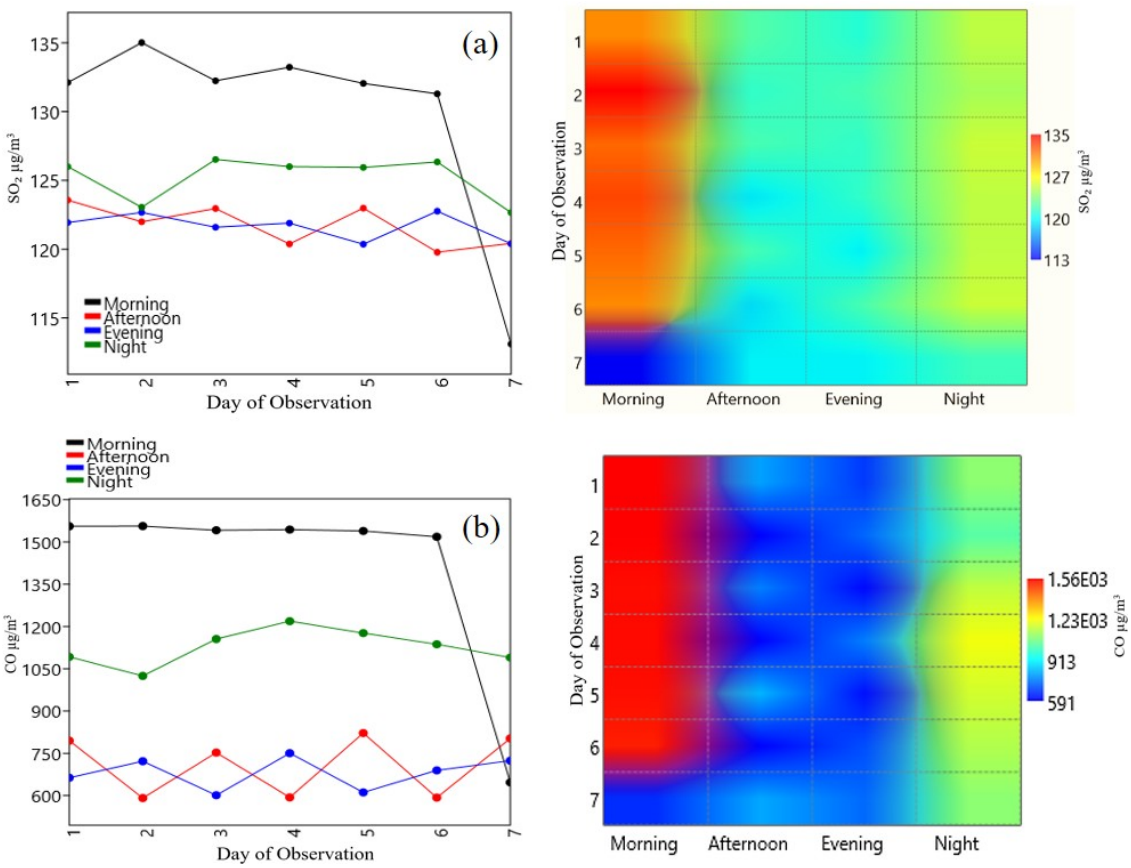

Figure 6. Distribution Variation and Heat Map of Daily Concentration Distribution Pattern Based on AQMS (a) Sulfur Dioxide (SO_2) (b) Carbon Monoxide (CO)

3.2 Pollutants Dispersion

Dispersion simulations using the AERMOD software were also conducted to analyze the direction and distribution patterns of pollutants originating from traffic activities along Jalan Sudirman. Through this modeling approach, a spatial representation was obtained, illustrating how emissions from motor vehicles are dispersed in the atmosphere and influence ambient air quality in the surrounding area.

On the first day of simulation, the prevailing wind direction was identified as blowing toward the northeast to east-northeast. This condition aligns with the dispersion modeling results generated using AERMOD, which show that the dispersion patterns of SO_2 and CO pollutants also move toward that sector. The highest concentrations (indicated by red areas) were detected around Sudirman Street, corresponding to zones of dense traffic activity Figure 8(a). Subsequently, Figure 8(b) illustrates the dispersion pattern on the second day, when the dominant wind direction shifted toward the north to north-northeast. The AERMOD dispersion modeling results were consistent with this wind pattern, showing pollutant plumes following the airflow. The highest concentrations of SO_2 and CO (indicated in red) were again concentrated around Jalan Sudirman, reflecting the area's status as the primary source of vehicular emissions.

On the third and fourth days, as illustrated in Figure 9, the dispersion patterns of both pollutants SO_2 and CO exhibited a dominant movement toward the north northeast to east. This pattern aligns consistently with the windrose data for the same period, which indicate that the prevailing winds originated from the west to southwest sectors. Similar to the previous days, the highest concentrations of both pollutants remained concentrated around Jalan Sudirman, which serves as the primary emission source due to the area's high traffic density.

Figure 10. present the dispersion modeling results of SO_2 and CO using AERMOD for days 5, 6 and 7, each compared with the corresponding daily windrose patterns. Figure 10(a) shows, the prevailing wind direction was toward the northeast to east, and the modeled dispersion pattern closely aligned with this direction. The highest concentrations of SO_2 and CO (indicated by red and yellow zones) were detected around Jalan Sudirman, the main corridor of traffic activity. Furthermore, the conditions on Day 6, as depicted in Figure 10(b), the dominant wind direction shifted toward the north-northeast, and the modeled dispersion results remained consistent with this shift. The

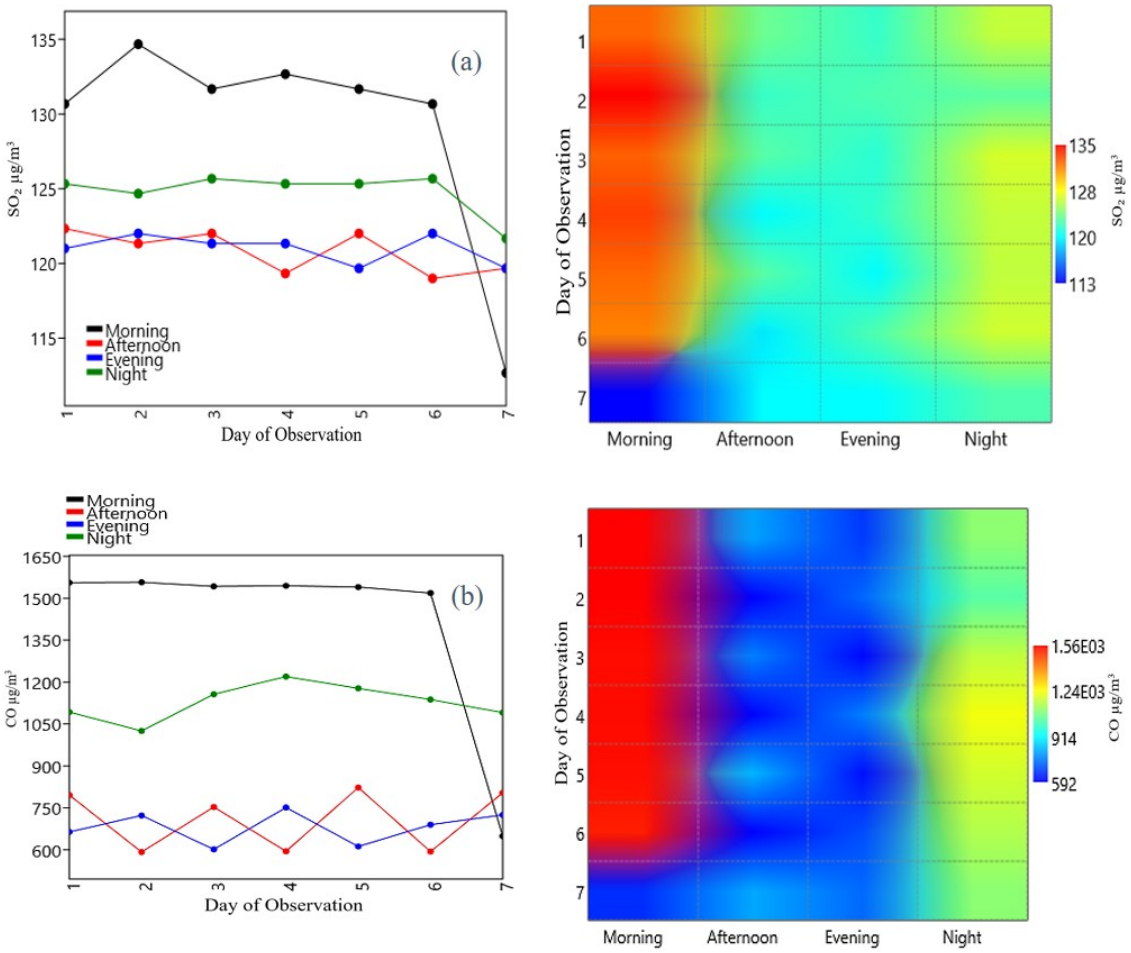

Figure 7. Distribution Variation and Heat Map of Daily Concentration Distribution Pattern Based on Empirical Measurement (a) Sulfur Dioxide (SO_2) (b) Carbon Monoxide (CO)

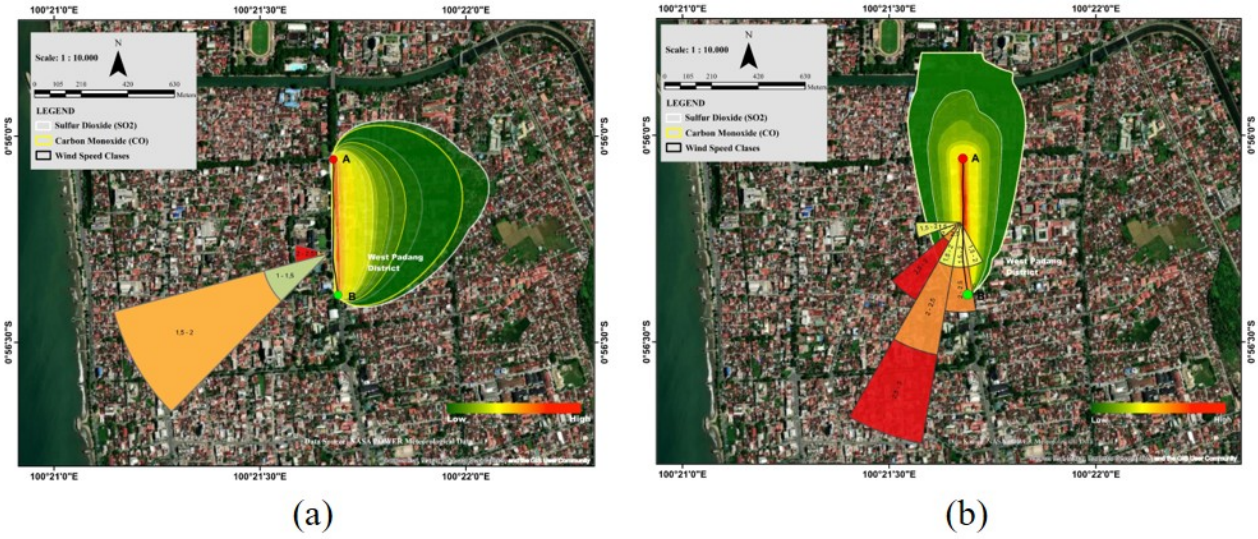

Figure 8. (a) Day 1 Dispersion Simulation (b) Day 2 Dispersion Simulation of SO_2 and CO Pollutants

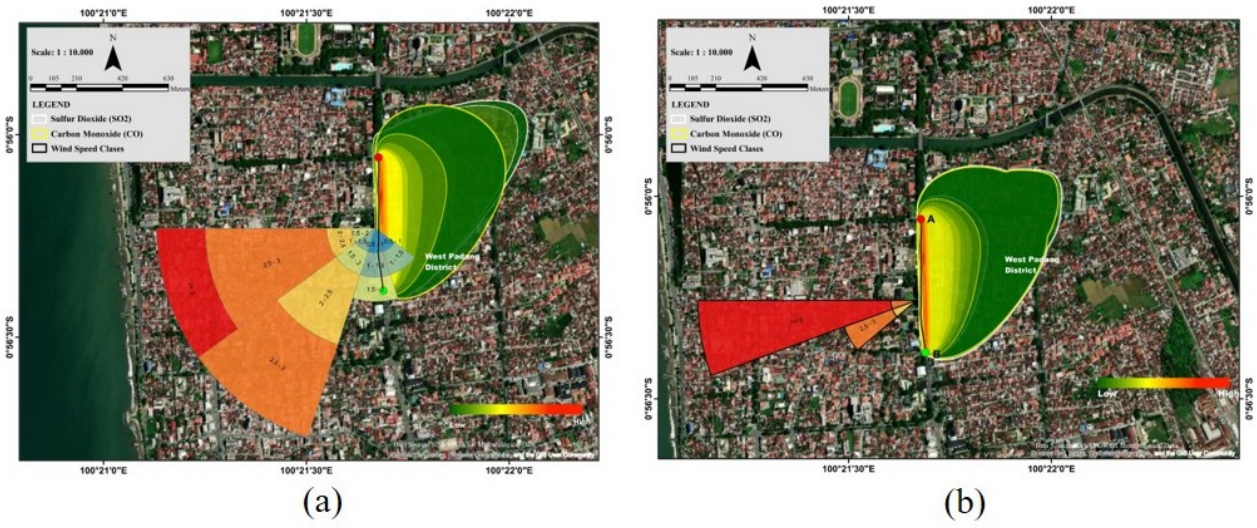

Figure 9. (a) Day 3 Dispersion Simulation (b) Day 4 Dispersion Simulation of SO_2 and CO Pollutants

pollutant plumes extended toward the northern part of the study area, although the highest concentrations continued to cluster near the primary emission source. Meanwhile for Day 7, as shown in Figure 10(c), the wind direction remained relatively stable, trending northward, and the dispersion patterns showed similar characteristics to the previous day. The maximum concentrations of SO_2 and CO were still concentrated around Jalan Sudirman, with slightly lower intensity compared to the preceding two days.

Based on the windrose analysis and dispersion patterns, wind speed and direction play a crucial role in determining the dynamics of pollutant dispersion in the atmosphere. Higher wind speeds generally enhance horizontal dispersion, thereby reducing pollutant concentrations near the ground surface. Conversely, weak wind conditions can slow down the dispersion process, leading to pollutant accumulation around emission sources (Faulkner et al., 2008; Matthew et al., 2019). Thus, spatial and temporal variations in wind speed and direction are key factors in explaining the differences observed between simulated and measured pollutant concentration patterns in the field.

3.3 Statistical Assessment

To evaluate the accuracy of pollutant concentration results simulated by AERMOD against data obtained from the Air Quality Monitoring System (AQMS) and direct field measurements using a Gas Impinger Sampler, a statistical analysis was conducted to assess the relationship and determine the error level between the model outputs and both AQMS and field measurement data.

The boxplot comparison results reveal consistent differences in the range and variability of pollutant concentrations between the AERMOD simulation outputs and observational data (both AQMS and field measurements). For sulfur dioxide (SO_2), the AERMOD simulation produced a wider concentration range of 100–150 $\mu g/m^3$, compared to the narrower observed range of 120–130 $\mu g/m^3$ (see Figure 11(a)). A similar pattern was observed for carbon monoxide (CO), where AERMOD estimated concentrations up to 2500 $\mu g/m^3$, in contrast to the more limited observed range of 800–1500 $\mu g/m^3$ as shown in Figure 11(b). Collectively, these findings suggest that AERMOD tends to generate higher maximum concentration estimates and greater variability compared to actual field measurements.

The boxplot analysis reveals that the model CO concentrations exhibit a substantially wider range compared to SO_2 when compared with both AQMS data and direct field measurements. This pattern is consistent with findings from several other urban studies, where model CO levels often exceed local air quality standards. Such results underscore the importance of accurate emission inventories and traffic data as input parameters, as inaccuracies in these factors can lead to significant discrepancies between simulated outcomes and actual field conditions (Macêdo and Ramos, 2020; Putranto et al., 2025).

Figure 12 illustrate the relationship between sulfur dioxide (SO_2) concentrations simulated by AERMOD and those obtained from observations (AQMS data and field measurements). Overall, both plots demonstrate an increasing trend in modeled SO_2 concentrations corresponding to higher observed values, indicating a positive correlation between AERMOD outputs and AQMS measurements, as evidenced by the upward-sloping red regression line. The relatively consistent data distribution within the concentration range of 115–135 $\mu g/m^3$ suggests a moderate linear relationship between the modeled and observed results, although variations among individual data points imply potential influences from meteorological factors or uncertainties in the model input parameters affecting the simulation outcomes.

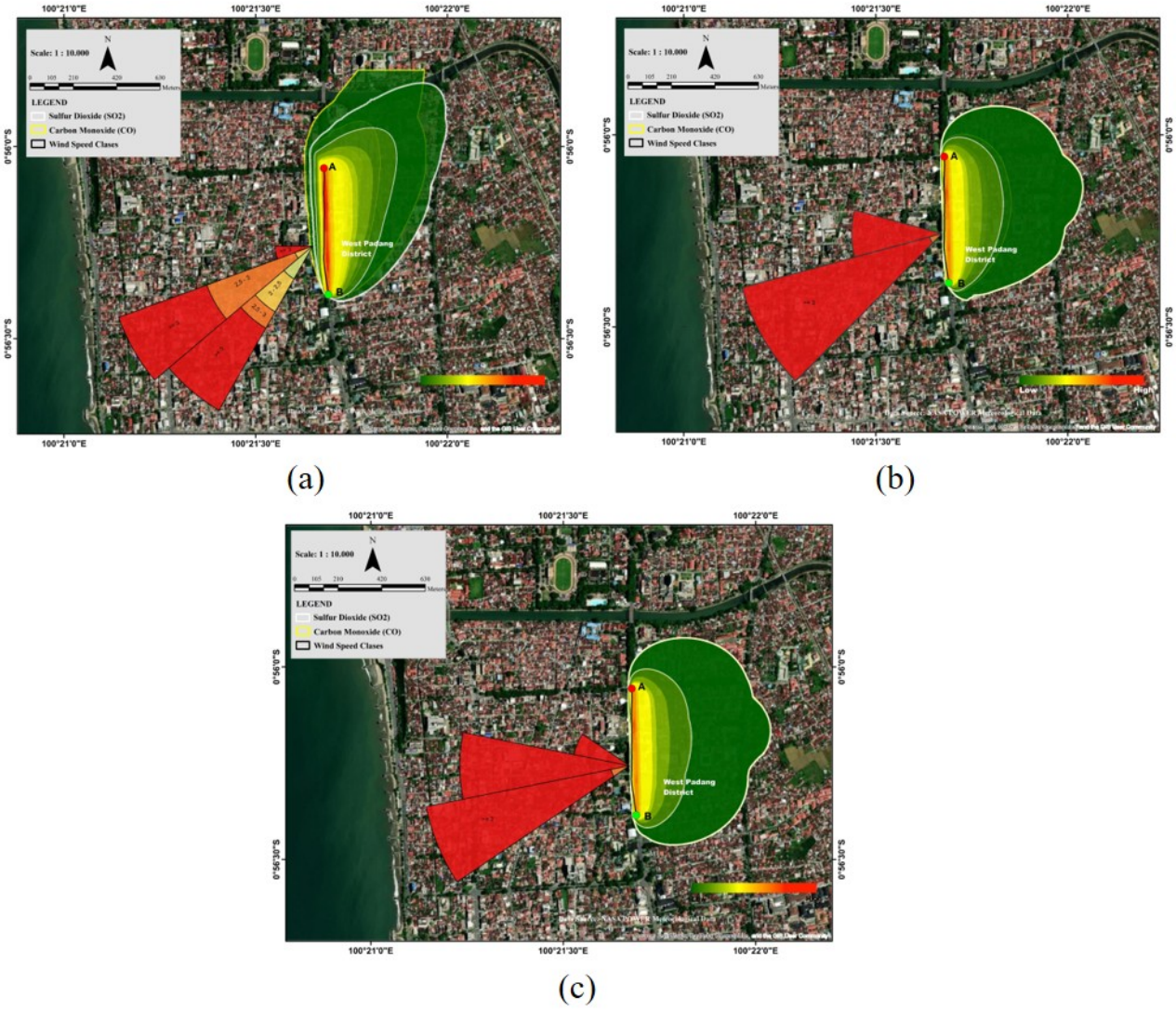

Figure 10. Day 5 Dispersion Simulation (b) Day 6 Dispersion Simulation (c) Day 7 Dispersion Simulation of SO_2 and CO Pollutants

The regression analysis between modeled carbon monoxide (CO) concentrations from AERMOD and observational data, as presented in Figure 13, reveals a positive relationship, albeit with a relatively low degree of correlation. The positively sloped regression line indicates that increases in observed CO values tend to correspond with higher simulated CO concentrations, although not in a strictly proportional manner. The wide dispersion of data points within the 600–1650 $\mu g/m^3$ range highlights considerable variability between AERMOD simulations and field measurements. Nevertheless, the overall trend suggests that AERMOD effectively captures the general direction of CO concentration changes in the atmosphere.

Several statistical indicators namely the Pearson correlation coefficient, MAE, NMSE, and RMSE were employed to evaluate the relationship, accuracy, and error magnitude between the simulated and observed data. These metrics collectively provide a comprehensive assessment of the model's capability to represent the observed variability in ambient pollutant concentrations.

The validation results indicate a distinct variation in AERMOD's performance for the two pollutants, as illustrated in the Table 4. For SO_2, the model performs satisfactorily, as evidenced by a strong and statistically significant positive correlation (Pearson = 0.61, p <0.001). Model accuracy is also high, reflected by a low MAE (13.7) and a very small NMSE (0.0378). Taken together, these statistical indicators confirm that AERMOD is able to consistently reproduce the observed SO_2 concentration trends. In contrast, the model's performance for CO is substantially weaker. The correlation is statistically insignificant (Pearson = 0.30, p = 0.20), accompanied by a very large estimation error (MAE

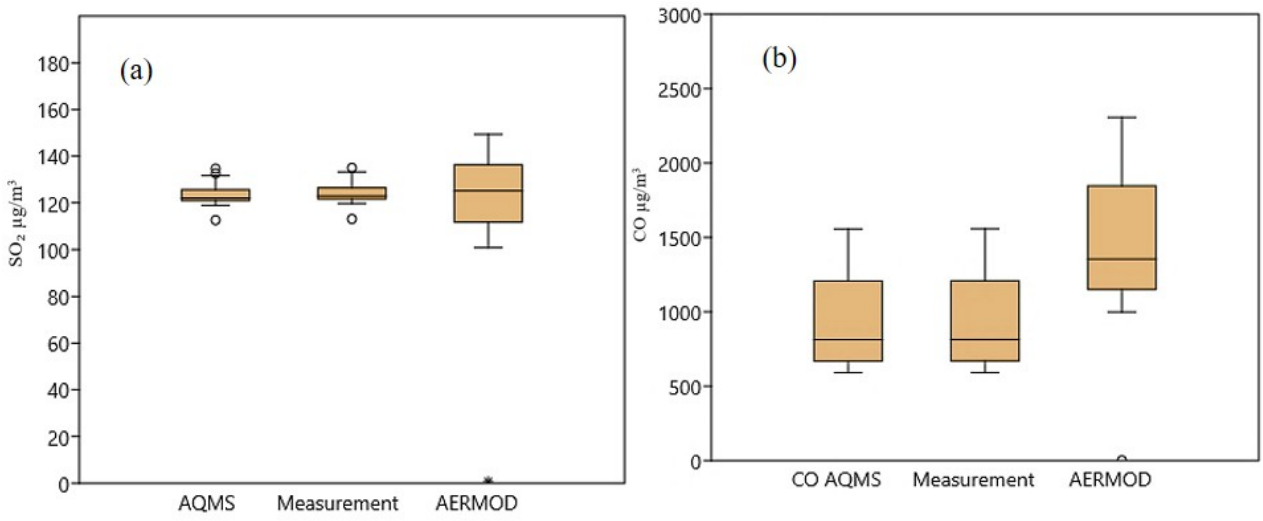

Figure 11. Boxplot of SO_2 and (b) Boxplot of CO for AERMOD Simulations, AQMS Data, and Field Measurements

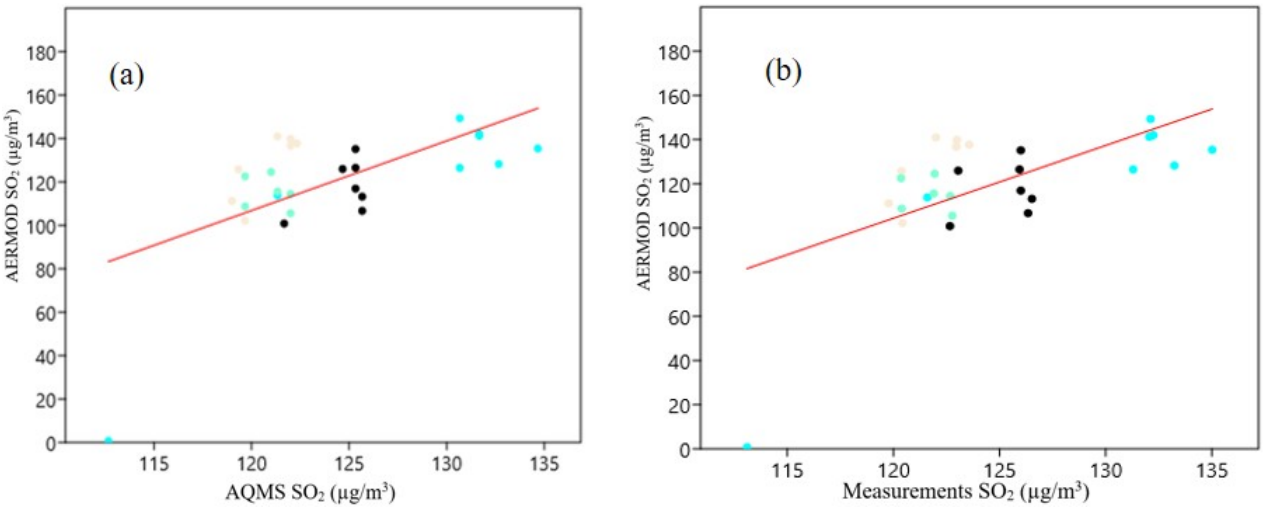

Figure 12. (a) Regression Analysis AERMOD and AQMS (b) Regression Analysis AERMOD and Empirical Measurement of SO_2

= 696.7) and a high NMSE (0.3465). These results indicate that AERMOD fails to capture the temporal dynamics of CO accurately. This discrepancy may be attributable to the nature of CO, which is highly sensitive to short-term traffic variability and urban micro-meteorological conditions, or potentially to inaccuracies within the emission inventory employed for the simulation.

These statistical findings are consistent with numerous studies demonstrating that the AERMOD dispersion model provides adequate performance in predicting sulfur dioxide (SO_2) concentrations originating from traffic-related emissions over long-term temporal scales, such as monthly to annual periods. This trend is particularly evident in studies conducted in Ghana and Thailand, where AERMOD outperformed CALPUFF in estimating SO_2 concentrations especially at higher concentration ranges and showed strong agreement with observational data on both annual and monthly timescales (Amoatey et al., 2019; Jittra et al., 2015). AERMOD's robust performance is further supported by studies from Indonesia, particularly in Tuban, East Java, where SO_2 predictions in semi-urban environments exhibited high accuracy. Krisbiantoro et al. (2022) reported values of mean absolute percent error (MAPE) and relative mean bias were below 10% across all grid resolutions, indicating a slight tendency toward underprediction but remaining well within acceptable error thresholds for regulatory and air quality management applications. These findings suggest that AERMOD offers reliable performance for model-based assessment and decision-making processes in such regions.

For carbon monoxide (CO), the model's performance

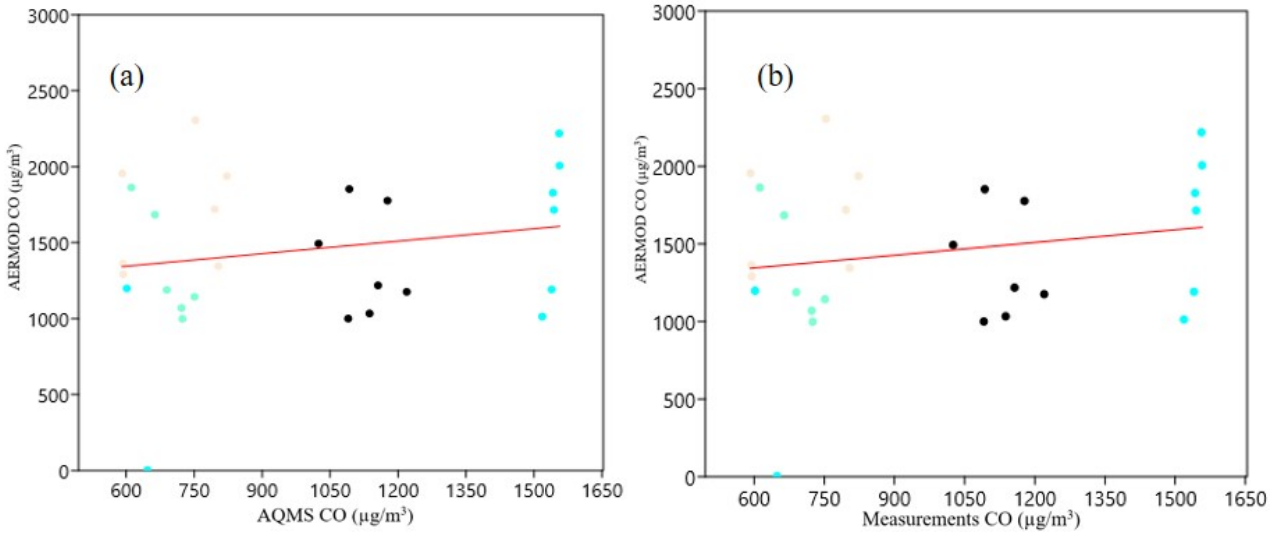

Figure 13. (a) Regression Analysis AERMOD and AQMS (b) Regression Analysis AERMOD and Empirical Measurement of CO

falls within a moderate category and exhibits a tendency toward overestimation, which is consistent with findings from studies conducted in regions with similar meteorological conditions. In Nairobi, for example, modeled CO concentrations reached 319 µg/m³, representing approximately 55% of the measured values (Matara et al., 2024). Consequently, while AERMOD can be effectively utilized for scenario analysis and dispersion pattern mapping of CO, the model still carries a higher level of uncertainty compared to other pollutants, particularly those that are highly sensitive to micro-meteorological variations, such as CO.

4. CONCLUSIONS

Analysis of AQMS data and field measurements revealed consistent diurnal patterns for SO_2 and CO along Jenderal Sudirman Street, with elevated concentrations during morning and nighttime hours and reduced levels from midday to afternoon. A notable anomaly occurred on the seventh day, when morning concentrations dropped drastically to their lowest recorded levels. Overall, the temporal patterns predicted by AERMOD were reasonably consistent with observational data, particularly during the morning period, although minor discrepancies were observed during midday, afternoon, and nighttime hours. Statistical evaluation indicates that AERMOD performs well in predicting SO_2, as reflected by strong and statistically significant Pearson correlations ($r = 0.60$; $p < 0.001$) and low MAE, NMSE, and RMSE values. In contrast, the model shows weaker performance for CO, with lower and non-significant correlations ($r = 0.30$; $p = 0.20$) as well as substantially higher MAE, NMSE, and RMSE values, reflecting the influence of emission variability and unresolved micro-meteorological conditions. Overall, AERMOD shows significant potential as an alternative monitoring tool in regions with limited AQMS infrastructure. When integrated with high-resolution meteorological data and field observations, the model provides a comprehensive framework for urban air quality assessment and offers a robust scientific foundation for evidence-based pollution mitigation policies.

ACKNOWLEDGEMENT

This research was funded by Directorate of Research and Community Service, Directorate General of Research and Development, Ministry of Higher Education, Science, and Technology, Under the Master's Thesis Research Scheme, In accordance with Research Contract Number: 060/C3/DT.05.00 /PL/2025, Fiscal Year 2025.

REFERENCES

Aboelkhair, H., M. Morsy, and G. El Afandi (2019). Assessment of Agroclimatology NASA POWER Reanalysis Datasets for Temperature Types and Relative Humidity at 2 m against Ground Observations over Egypt. *Advances in Space Research*, **64**(1); 129–142

Ajnoti, N., H. Gehlot, and S. N. Tripathi (2024). Hybrid Instrument Network Optimization for Air Quality Monitoring. *Atmospheric Measurement Techniques*, **17**(6); 1651–1664

Amoatey, P., H. Omidvarborna, H. A. Affum, and M. Baawain (2019). Performance of AERMOD and CALPUFF Models on SO_2 and NO_2 Emissions for Future Health Risk Assessment in Tema Metropolis. *Human and Ecological Risk Assessment*, **25**(3); 772–786

Chandler, W. S., J. M. Hoell, D. Westberg, T. Zhang, and P. W. Stackhouse (2013). *NASA Prediction of Worldwide*

Energy Resource High Resolution Meteorology Data for Sustainable Building Design. NASA, Baltimore, USA

Chen, T.-M., W. G. Kuschner, J. Gokhale, and S. Shofer (2007). Outdoor Air Pollution: Nitrogen Dioxide, Sulfur Dioxide, and Carbon Monoxide Health Effects. *The American Journal of the Medical Sciences*, **333**(4); 249–256

Chen, Z., N. Liu, H. Tang, X. Gao, Y. Zhang, H. Kan, F. Deng, B. Zhao, X. Zeng, Y. Sun, H. Qian, W. Liu, J. Mo, X. Zheng, C. Huang, C. Sun, and Z. Zhao (2022). Health Effects of Exposure to Sulfur Dioxide, Nitrogen Dioxide, Ozone, and Carbon Monoxide between 1980 and 2019: A Systematic Review and Meta-Analysis. *Indoor Air*, **32**(11); e13170

Cimorelli, A. J., S. G. Perry, A. Venkatram, J. C. Weil, R. J. Paine, R. B. Wilson, R. F. Lee, W. D. Peters, and R. W. Brode (2005). AERMOD: A Dispersion Model for Industrial Source Applications. Part I: General Model Formulation and Boundary Layer Characterization. *Journal of Applied Meteorology*, **44**(5); 682–693

Colvile, R. N., E. J. Hutchinson, J. S. Mindell, and R. F. Warren (2001). The Transport Sector as a Source of Air Pollution. *Atmospheric Environment*, **35**(9); 1537–1565

Craig, K. J., L. M. Baringer, S.-Y. Chang, M. C. McCarthy, S. Bai, A. F. Seagram, V. Ravi, K. Landsberg, and D. S. Eisinger (2020). Modeled and Measured Near-Road PM2.5 Concentrations: Indianapolis and Providence Cases. *Atmospheric Environment*, **240**; 117775

Demirarslan, K. O. (2025). Effects of Topographic Variables on Traffic-Related Pollutant Concentrations: Comparison of AERMOD and CAL3QHCR Models. *Frontiers in Environmental Science*, **13**; 1577330

Dobson, R., K. Siddiqi, T. Ferdous, R. Huque, M. Lesosky, J. Balmes, and S. Semple (2021). Diurnal Variability of Fine-Particulate Pollution Concentrations: Data from 14 Low- and Middle-Income Countries. *The International Journal of Tuberculosis and Lung Disease*, **25**(3); 206–214

Faulkner, W. B., B. W. Shaw, and T. Grosch (2008). Sensitivity of Two Dispersion Models (AERMOD and ISCST3) to Input Parameters for a Rural Ground-Level Area Source. *Journal of the Air & Waste Management Association*, **58**(10); 1288–1296

Herath Bandara, S. J. and N. Thilakarathne (2025). Economic and Public Health Impacts of Transportation-Driven Air Pollution in South Asia. *Sustainability*, **17**(5); 2306

Hura, V. and O. Dutsiak (2024). Optimising the Network of Air Quality Monitoring Stations. *Artificial Intelligence*, **29**(2); 72–84

Hussain, M., S. Aleem, A. Karim, F. Ghazanfar, M. Hai, and K. Hussain (2020). Design of Low Cost, Energy Efficient, IoT Enabled, Air Quality Monitoring System with Cloud Based Data Logging, Analytics and AI. In *2020 International Conference on Emerging Trends in Smart Technologies (ICETST)*. IEEE, Karachi, Pakistan, pages 1–6

Irankunda, E., Z. Török, A. Mereuţă, J. Gasore, E. Kalisa, B. Akimpaye, T. Habineza, O. Shyaka, G. Munyampundu, and A. Ozunu (2022). The Comparison between In-Situ Monitored Data and Modelled Results of Nitrogen Dioxide (NO2): Case-Study, Road Networks of Kigali City, Rwanda. *Heliyon*, **8**(12); e12390

Jittra, N., N. Pinthong, and S. Thepanondh (2015). Performance Evaluation of AERMOD and CALPUFF Air Dispersion Models in Industrial Complex Area. *Air, Soil and Water Research*, **8**; ASWR.S32781

Kiribou, I. A. R., T. Neya, B. Nana, K. Ogunjobi, T. Daho, Y. W. Gounkaou, F. M. Muema, and D. W. Sintayehu (2025). Road Transport and Urban Mobility Greenhouse Gas Emissions Factor for Air Pollution Modeling in Burkina Faso. *Journal of Urban Mobility*, **7**; 100106

Krisbiantoro, A., A. D. Syafei, and A. F. Assomadi (2022). Computational Pollutant Dispersion of SO_2/NO_2 in the Environment Using AERMOD in a Semi-Urban Area: A Case Study in Tuban, East Java. *International Journal of Advanced Research*, **10**(2); 670–675

Kumar, A., S. Dixit, C. Varadarajan, A. Vijayan, and A. Masuraha (2006). Evaluation of the AERMOD Dispersion Model as a Function of Atmospheric Stability for an Urban Area. *Environmental Progress*, **25**(2); 141–151

Kumar, A., I. P. Singh, and S. K. Sud (2011). Energy Efficient Air Quality Monitoring System. In *2011 IEEE Sensors Proceedings*. IEEE, Limerick, Ireland, pages 1562–1566

Kumar, M. V., S. A. Ram, M. Wasim, H. Gupta, and M. V. Krishna (2021). Smart Air Quality Monitoring System in Realtime Using IoT. *Turkish Journal of Computer and Mathematics Education*, **12**(10); 1965–1969

Lee, J., J.-W. Hong, K. Lee, J. Hong, E. Velasco, Y. J. Lim, J. B. Lee, K. Nam, and J. Park (2019). Ceilometer Monitoring of Boundary-Layer Height and Its Application in Evaluating the Dilution Effect on Air Pollution. *Boundary-Layer Meteorology*, **172**(3); 435–455

Macêdo, M. F. M. and A. L. D. Ramos (2020). Vehicle Atmospheric Pollution Evaluation Using AERMOD Model at Avenue in a Brazilian Capital City. *Air Quality, Atmosphere & Health*, **13**(3); 309–320

Matara, C., S. Osano, A. Yusuf, and E. Akech (2024). An Assessment of the Contribution of Vehicular Traffic to Ambient Air Quality: A Case Study of Nairobi Expressway Corridor. *Civil and Environmental Engineering*, **20**(1); 54–67

Matthew, O. J., A. N. Igbayo, F. S. Olise, K. O. Owoade, O. E. Abiye, M. A. Ayoola, and P. K. Hopke (2019). Simulation of Point Source Pollutant Dispersion Pattern: An Investigation of Effects of Prevailing Local Weather Conditions. *Earth Systems and Environment*, **3**(2); 215–230

Ministry of Enviroment (2010). *Ministry of Environment of the Republic of Indonesia Regulation of the Minister of Environment of the Republic of Indonesia Number 12*

of 2010 on the Implementation of Air Pollution Control. Government of Indonesia

Mohan, M., S. Bhati, A. Sreenivas, and P. Marrapu (2011). Performance Evaluation of AERMOD and ADMS-Urban for Total Suspended Particulate Matter Concentrations in Megacity Delhi. *Aerosol and Air Quality Research*, **11**(7); 883–894

Oke, T. R., G. Mills, A. Christen, and J. A. Voogt (2017). *Urban Climates*. Cambridge University Press, United Kingdom

Putranto, A. W., M. Z. Arifin, F. R. Sutikno, H. Bowoputro, and M. Miftahulkhair (2025). Modeling of Carbon Monoxide Emission Dispersion of Vehicles in Malang City Using AERMOD. *EUREKA: Physics and Engineering*, (2); 188–198

Qi, X., G. Mei, S. Cuomo, C. Liu, and N. Xu (2021). Data Analysis and Mining of the Correlations between Meteorological Conditions and Air Quality: A Case Study in Beijing. *Internet of Things*, **14**; 100127

Rezaali, M., R. Fouladi-Fard, P. O'Shaughnessy, K. Naddafi, and A. Karimi (2025). Assessment of AERMOD and ADMS for NOx Dispersion Modeling with a Combination of Line and Point Sources. *Stochastic Environmental Research and Risk Assessment*, **39**(2); 813–827

Singh, A., D. Ng'ang'a, M. J. Gatari, A. W. Kidane, Z. A. Alemu, N. Derrick, M. J. Webster, S. E. Bartington, G. N. Thomas, W. Avis, and F. D. Pope (2021). Air Quality Assessment in Three East African Cities Using Calibrated Low-Cost Sensors with a Focus on Road-Based Hotspots. *Environmental Research Communications*, **3**(7); 075007

Snyder, M. G., A. Venkatram, D. K. Heist, S. G. Perry, W. B. Petersen, and V. Isakov (2013). RLINE: A Line Source Dispersion Model for Near-Surface Releases. *Atmospheric Environment*, **77**; 748–756

Sobieraj, K., S. Stegenta-Dkabrowska, G. Luo, J. A. Koziel, and A. Białowiec (2022). Carbon Monoxide Fate in the Environment as an Inspiration for Biorefinery Industry: A Review. *Frontiers in Environmental Science*, **10**; 822463

Stull, R. B. (1988). *An Introduction to Boundary Layer Meteorology*. Kluwer Academic, Netherlands

Su, T., Z. Li, and R. Kahn (2018). Relationships between the Planetary Boundary Layer Height and Surface Pollutants Derived from Lidar Observations over China: Regional Pattern and Influencing Factors. *Atmospheric Chemistry and Physics*, **18**(21); 15921–15935

Suhito, I. R., K.-M. Koo, and T.-H. Kim (2020). Recent Advances in Electrochemical Sensors for the Detection of Biomolecules and Whole Cells. *Biomedicines*, **9**(1); 15

Tamin, O. Z. (2008). *Perencanaan dan Pemodelan Transportasi*. Penerbit ITB Bandung

Thepanond, S. (2016). Evaluation of Dispersion Model Performance in Predicting SO_2 Concentrations from Petroleum Refinery Complex. *International Journal of GEOMATE*, **11**(23); 2365–2372

Tun, S. N. L., T. H. Aung, A. S. Mon, P. H. Kyaw, W. Siriwong, M. Robson, and T. Htut (2018). Assessment of Ambient Dust Pollution Status at Selected Point Sources (Residential and Commercial) of Mingaladon Area, Yangon Region, Myanmar. *Journal of Health Research*, **32**(1); 60–68

Verma, R. L., N. T. K. Oanh, E. Winijkul, L. N. Huy, I. P. Armart, W. Laowagul, S. Sooktawee, D. A. Permadi, M. F. Khan, L. Gunawardhana, and M. K. Patdu (2023). Air Quality Management Status and Needs of Countries in South Asia and Southeast Asia. *APN Science Bulletin*, **13**(1); 102

Xu, Z., L. Xiong, D. Jin, and J. Tan (2021). Association between Short-Term Exposure to Sulfur Dioxide and Carbon Monoxide and Ischemic Heart Disease and Non-Accidental Death in Changsha City, China. *PLOS ONE*, **16**(5); e0251108

Zheng, H. (2009). Design and Application for Environmental Air Quality Automatic Monitoring System. In *2009 9th International Conference on Electronic Measurement & Instruments*. IEEE, Beijing, China, pages 218–221

